7th International Conference on Silicon Photovoltaics, SiliconPV 2017

Investigation of atomic-layer-deposited TiO$_x$ as selective electron and hole contacts to crystalline silicon

Takuya Matsui[a,b,]*, Martin Bivour[a], Paul Ndione[a,c], Paul Hettich[a] and Martin Hermle[a]

[a] Fraunhofer Institute for Solar Energy Systems ISE, Heidenhofstrasse 2, Freiburg 79110, Germany
[b] National Institute of Advanced Industrial Science and Technology, 1-1-1 Umezono, Tsukuba 305-8568, Japan
[c] National Renewable Energy Laboratory, 15013 Denver West Parkway, Golden, CO 80401, USA

Abstract

The applicability of atomic-layer-deposited titanium oxide (TiOx) thin films for the formation of carrier selective contacts to crystalline silicon (c-Si) is investigated. While relatively good electron selectivity was presented recently by other groups, we show that carrier selectivity can be engineered from electron to hole selective depending on the deposition conditions, post deposition annealing and the contact material covering the TiOx layer. For both the electron and hole contacts, an open-circuit voltage (Voc) of ~ >650 mV is obtained. The fact that the Voc is correlated with the (asymmetric) induced c-Si band bending suggests that carrier selectivity is mainly governed by the effective work function and/or the fixed charge rather than by the asymmetric band offsets at the Si/TiOx interface, which provides important insight into the basic function of metal-oxide-based contact systems.

1. Introduction

Carrier selective contact that extracts one type of carrier (electron or hole) out of the light-absorbing material is a subject of current interest for photovoltaic application [1]. In particular, novel carrier selective contacts for crystalline silicon (c-Si) can be used to replace the conventional p-n homojunction and hydrogenated amorphous

* Corresponding author. Tel.: +81-29-861-3204; fax: +81-29-861-3367.
  E-mail address: t-matsui@aist.go.jp

silicon (a-Si:H)/c-Si heterojunction schemes for achieving high efficiency without complex device processing. While various high-work-function transition-metal-oxides such as MoO_x, WO_x, and V_2O_x have been demonstrated as hole selective contacts for c-Si solar cells [2-4], efficient electron selective contact has been lacking. Recently, TiO_x (or TiO_2) thin-layers deposited by atomic layer deposition (ALD) [5] or chemical vapor deposition [6,7] have been reported to act as electron selective contacts to crystalline silicon solar cells. Yang *et al*. demonstrated a 21.6% efficient solar cell by applying a thermal-ALD TiO_x to full-area rear electron contact for N-type monocrystalline silicon base [5]. The origin of the electron selectivity of TiO_x has been ascribed to the asymmetric current flow at the Si/TiO_x interface where the low conduction band offset allows the electron flow while the high valence band offset hinders the hole flow [5-7]. Meanwhile, it is suggested that ALD-TiO_x contain negative fixed charge [8,9], which might be detrimental in aiming for an ideal electron selective contact. In this work, we have investigated the carrier selectivity of TiO_x prepared by ALD with different oxidation processes using oxygen plasma and thermal reaction with H_2O vapor. Our results show that the carrier selectivity of TiO_x is widely tunable from electron-selective (V_{oc}~680 mV) to hole-selective (V_{oc}~650 mV) by the ALD process, post-deposition treatments and contact material that covers TiO_x layer.

2. Experiment

We fabricated solar cell precursors as shown in Fig. 1. Si wafers (N-type float zone silicon, 1 Ωcm, (100) orientation, 200 μm thick, planar surface) were RCA-cleaned and HF-dipped prior to deposition process. TiO_x was deposited by an ALD system (FlexAL, Oxford Instruments) on the rear-side of c-Si wafer. Titanium isopropoxide (TTIP) was used as a Ti precursor. The oxidation during every ALD cycle took place using either O_2 plasma or thermal reaction with H_2O vapor. We term these processes as plasma- and thermal-ALD, respectively. Although a substantially longer purge time was required after H_2O dose (30 s) than after O_2 plasma (2 s), TiO_x were deposited at a similar growth rate per cycle of ~0.045 nm in both ALD processes. In this study, to focus on the carrier selectivity of TiO_x, an intrinsic a-Si:H buffer layer (8-15 nm) was deposited by plasma-enhanced chemical vapor deposition prior to TiO_x. This buffer layer preserves the surface passivation quality unchanged regardless of the ALD condition, as confirmed by measuring the quasi-steady-state photoconductance (QSSPC) [10] before and after TiO_x deposition. As a rear contact after ALD-TiO_x, four different conductive materials (Ti, Al, Pd, and ITO) were examined. The front-side emitter or front-surface-field (FSF) was formed using a standard heterojunction structure (a-Si:H *i-p* or *i-n* stack), following a sputtered ITO layer [4]. As shown in Fig. 1, TiO_x acts either as electron contact and back-surface-field (BSF) or hole contact and rear-emitter for N-type base. Suns-V_{oc} measurement [11] was carried out before and after hotplate annealing at 180°C for 15 min in ambient air. Apart from solar cell precursors, TiO_x layers were directly
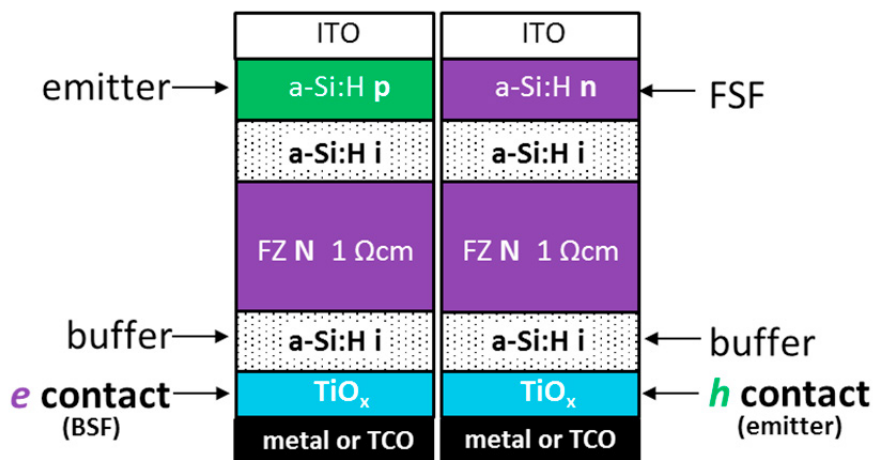

Fig. 1. Schematic illustration of sample structures studied in this work.

deposited on N- and P-type c-Si (1 Ωcm) to measure the induced c-Si band bending by using a surface photovoltage (SPV) technique with a 905-nm laser pulse [12,13].

3. Results and discussion

In Fig. 2, (a) the suns-V_{oc} curves (initial state only) and (b) the corresponding external 1-sun V_{oc} as a figure of merit of the carrier selectivity (both initial and annealed states) are depicted for the two different solar cell precursors shown in Fig. 1. A 6-nm-thick TiO_x layer was deposited on an intrinsic a-Si:H buffer layer either by plasma-ALD (red) or thermal-ALD (blue). For comparison, the results of the standard heterojunction solar cells, i.e., *pi*N*in* and *ni*N*ip*, are included. In this series, Ti was used as a rear electrode. Note that the positive V_{oc} in Fig. 2 (b) represents the magnitude of electron selectivity (TiO_x and a-Si:H *n*-layer as electron contacts) while the negative V_{oc} represents the hole selectivity (TiO_x and a-Si:H *p*-layer as hole contacts). As mentioned earlier, the intrinsic a-Si:H buffer layer between c-Si and TiO_x layer preserves excellent surface passivation, providing an implied V_{oc} at 1 sun illumination of about 720 mV after both plasma- and thermal-ALD TiO_x depositions. It can be seen in Fig. 2(b) that the V_{oc} for the doped a-Si:H references are very close to the implied V_{oc} (iV_{oc}), as expected for a contact featuring good selectivity [14]. Nevertheless, as shown in Figs. 2 (a) and (b), a pronounced variation in carrier selectivity is found for TiO_x contacts depending on the ALD process. It is observed that plasma-ALD TiO_x (red) exhibits electron selectivity rather than hole selectivity. On the other hand, thermal-ALD TiO_x (blue) exhibits rather hole selectivity. In fact, when using a thermal-ALD TiO_x as an electron contact, a negative slope in the suns-V_{oc} curve, i.e., decreasing voltage with
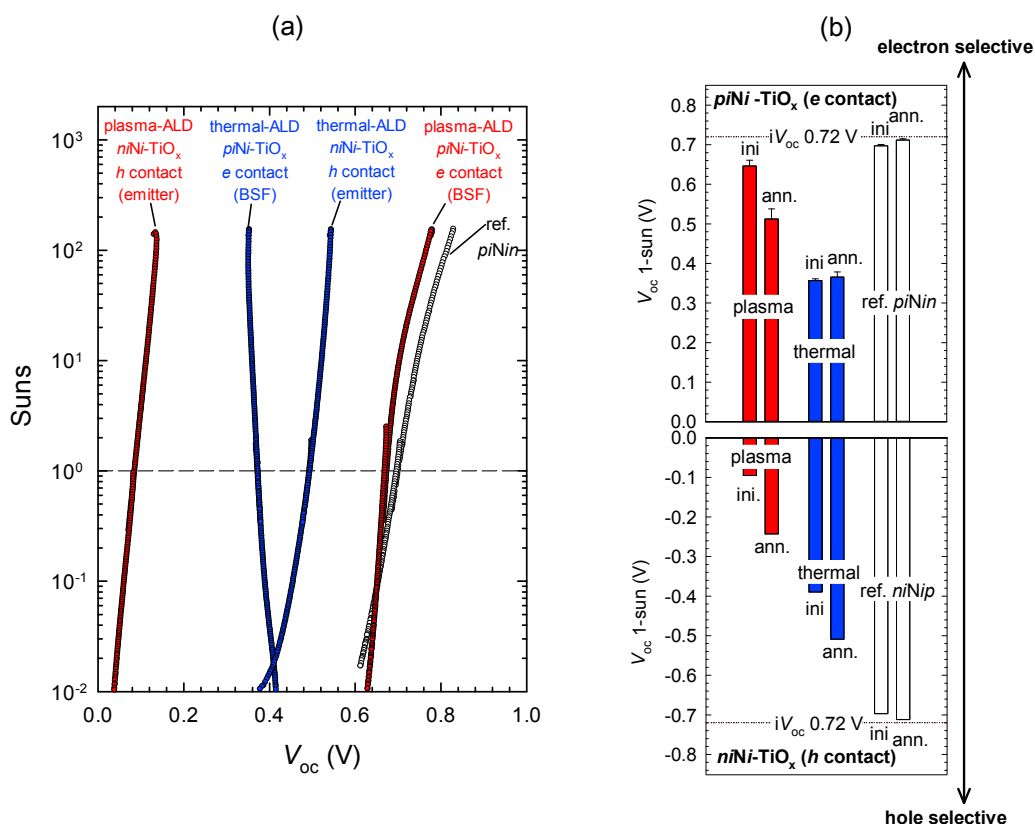

Fig. 2. (a) suns-V_{oc} curves (initial) and (b) external 1-sun V_{oc} in the initial (ini.) and after annealing (ann.) for different solar cell structures shown in Fig. 1. A 6-nm-thick TiO_x layer was deposited by either plasma- (red) or thermal-ALD (blue). The results of the standard heterojunction solar cells (white) are also shown for comparison. In (b), the positive and negative external V_{oc} represent the magnitude of electron and hole selectively, respectively.

increasing illumination intensity as shown in Fig. 2(a), is observed. This negative ideal factor (n<0) at low illuminations indicates the presence of a non-ideal contact characteristics with respect to extraction of the excess electrons from the absorber [14,15] by the a-Si:H(*i*)/TiO$_x$/Ti contact. As will be shown in the following by SPV measurements, this poor selectivity is closely linked to the induced c-Si band bending. Furthermore, it is seen in Fig. 2(b) that the post-deposition annealing declines the electron selectivity whereas it enhances the hole selectivity, except for the device with thermal-ALD TiO$_x$ used as electron contact. Although the mechanism behind this phenomenon is not well understood, we found that the impact of post-deposition annealing was the strongest when annealing the samples after TiO$_x$/capping layer (Ti, Al, Pd and ITO) stack compared to annealing before metallization (or TCO deposition). This suggests that some chemical reaction takes place at the TiO$_x$/capping layer interface, influencing the carrier selectivity. According to the paper by Yang *et al.* [5], a reduction reaction of the TiO$_x$ layer is occurred by the covering Al layer during annealing due to the stronger oxygen affinity of Al. However, they observed improved electron selectivity by post-deposition annealing, which is clearly opposite from our observation.

To gain insight into the origin of the different carrier selectivity of TiO$_x$, we measured SPV for the plasma- and thermal-ALD TiO$_x$ deposited on c-Si (N and P base) without a-Si:H(*i*) buffer layer. Figure 3(a) shows the induced c-Si band bending (Φ) measured by SPV for these samples before and after annealing. For comparison, the measured Φ for n- and p-type a-Si:H layers (~10 nm) deposited on c-Si are included. These doped a-Si:H contacts demonstrate an ideal band bending (>800 mV) when depositing them on c-Si base with asymmetric polarity, i.e., *n* on P and *p* on N. It is evident that plasma- and thermal-ALD induce the band bending in an opposite way, i.e., plasma-ALD TiO$_x$ induces greater band bending for P-base than for N-base while the thermal-ALD TiO$_x$ induces strong band bending (>800 mV) only for N-base. By plotting external V$_{oc}$ of solar cell precursors versus induced band bending measured by SPV, a correlation is found as shown in Fig. 3(b), indicating that the higher induced-band bending leads to the more efficient carrier selectivity.
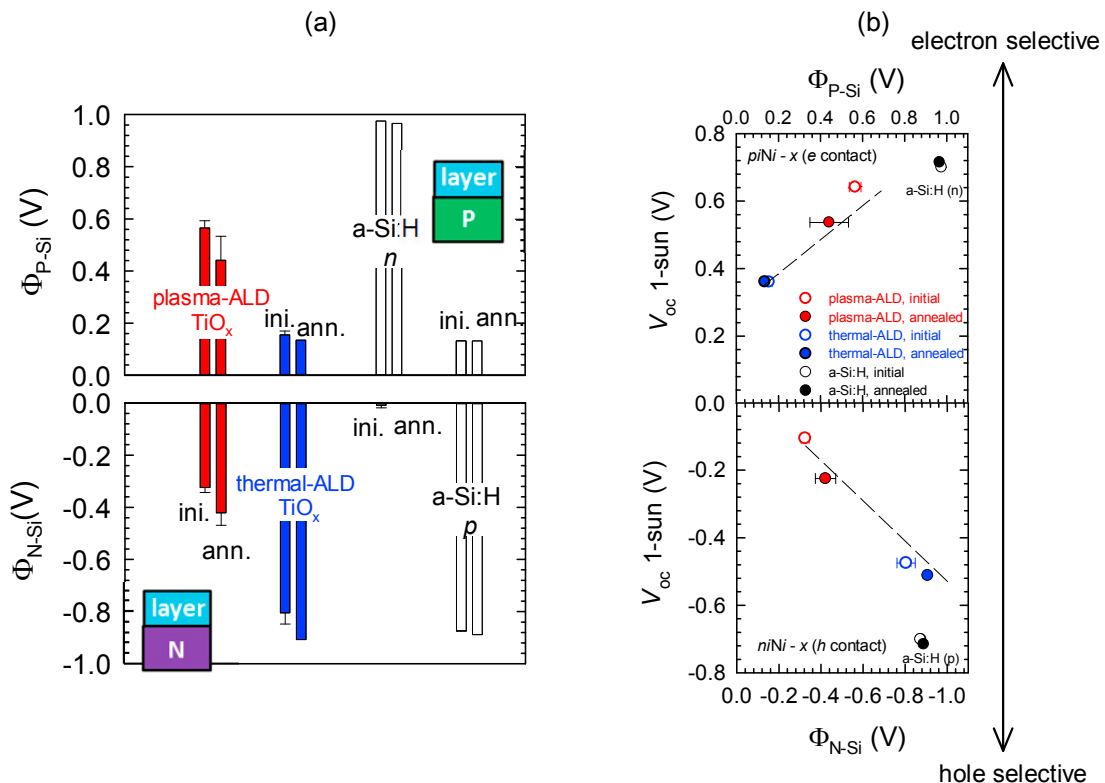

Fig. 3. (a) SPV signals (Φ) for TiO$_x$ layers deposited on P- (top) and N-type (bottom) c-Si in the initial (ini.) and annealed (ann.) states. TiO$_x$ was deposited by plasma- (red) or thermal-ALD (blue). For comparison, SPV signals for a-Si:H n and p layers are also shown. (b) V$_{oc}$ of *piNi-X* (*X* represents plasma/thermal-ALD TiO$_x$ or *p/n* a-Si:H) and *niNi-X* samples plotted versus Φ measured on P/*X* and N/*X* contacts, respectively. Open and closed symbols represent the initial and annealed states, respectively.

Further investigations revealed that the carrier selectivity of TiO_x is significantly influenced by the capping contact material. Figure 4 shows the 1-sun external V_{oc} for solar cell precursors with various contact materials (Ti, Al, ITO, Pd). In Fig. 4, to compare the maximum V_{oc} obtained from each solar cell structure, the V_{oc} of *initial* state are shown for plasma-ALD TiO_x used as an electron contact while those of *annealed* state are shown for thermal-ALD TiO_x used as a hole contact. As shown in Fig. 4, among four materials examined in this study, plasma-ALD TiO_x provides the highest electron selectivity when coating it with Al but the lowest one with Pd. An almost inverse behaviour is observed for the hole selectivity of the thermal-ALD TiO_x. By combining TiO_x with the best contact material, almost symmetric carrier selectivity from electron selective (V_{oc}~ 680 mV) to hole selective (V_{oc}~-650 mV) is obtained using the plasma-ALD TiO_x/Al stack and the thermal-ALD TiO_x/ITO stack, respectively. These results indicate that the c-Si band bending is influenced by the work function (WF) of the contact material, as WF of Al is the lowest but that of Pd is the highest among the materials investigated (Ti: 4.3 eV, Al: 4.2 eV, Pd: 5.4 eV [16], ITO: 4.8 eV [17]). Similarly, Allen *et al*. reported that the deposition of Ca as a low WF metal (<3 eV) on ALD-TiO_x led to an improved electron contact [18]. Based on these results, it is likely that the carrier density in TiO_x is too low so that the screening length of TiO_x layer is well above its thickness. An exception is found for thermal-ALD TiO_x/Pd stack, as it shows lower V_{oc} (~580 mV) than that with ITO (~650 mV). Since this TiO_x/Pd stack resulted in the highest *initial* V_{oc} (~630 mV, not shown in the figure), post-deposition annealing of TiO_x/Pd stack might degrade the contact properties.

Our results revealed that TiO_x can act as either electron or hole selective contact depending on ALD process and its selectivity is strongly influenced by the post-deposition annealing and WF of metal or TCO contact on top of TiO_x layer. Although the mechanism behind these findings is not yet understood, the band offset at Si/metal-oxide contact does not fully account for the observed carrier selectivity because our thermal-ALD TiO_x acts as hole selective contact despite of the presumed presence of large valence band offset at the Si/TiO_x interface. Rather than this, we propose
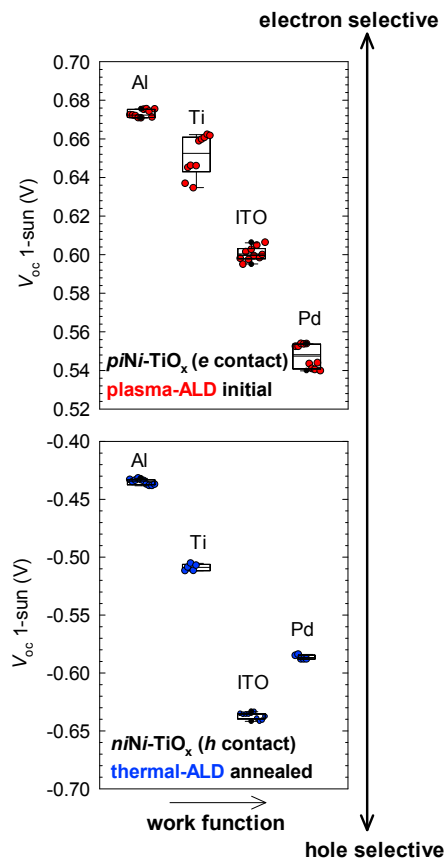

Fig. 4. Influence of capping material (Ti, Al, Pd and ITO) on top of TiO_x layer on external 1-sun V_{oc} of two solar cell precursors with plasma-ALD TiO_x as electron contact (top, initial state) and thermal-ALD TiO_x as hole contact (bottom, annealed state).

that an asymmetric band bending in c-Si induced by the difference of effective WF and/or fixed charge of metal-oxide contact gives more qualitative explanation for the observed carrier selectivity. Furthermore, we highlight that the need for a capping layer featuring a proper work function limits the applicability of TiO_x in practical contact systems, as high efficiency device requires not only good electrical contact but also proper optical design that often includes low-n transparent conductive oxide layer to minimize the optical absorption loss at the contact.

4. Conclusions

Although the carrier selectivity of our TiO_x is still behind the level of the doped a-Si:H, our results show that it is widely tunable from electron to hole contacts and can be further optimized by the choice of contact material. It can be considered that carrier selectivity of TiO_x is changed by the electrical properties of TiO_x, e.g., Fermi level / WF and fixed charge density. To give a more holistic view on the basic function of metal-oxide-based contact systems, the mechanism behind the tunable carrier selectivity of TiO_x and some design rules, simulation results and structural investigations comparing the hole and electron selective TiO_x films will be presented in the future. Further study is also ongoing to improve the carrier selectivity to the level of the doped a-Si:H layers.

Acknowledgements

References

[1] Würfel U, Cuevas A, Würfel P. Charge Carrier Separation in Solar Cells. IEEE J. Photovoltaics 2015; 5; 461-469.

[2] Battaglia C, Yin X, Zheng M, Sharp ID, Chen T, McDonnell S, Azcatl A, Carraro C, Ma B, Maboudian R, Wallace RM, Javey A. Hole selective MoO_x contact for silicon solar cells. Nano Lett. 2014; 14; 967-971.

[3] Gerling LG, Mahato S, Morales-Vilches A, Masmitja G, Ortega P, Voz C, Alcubilla R, Puigdollers J. Transition metal oxides as hole-selective contacts in silicon heterojunctions solar cells. Sol. Energy Mater. Sol. Cells 2016; 145; 109-115.

[4] Bivour M, Temmler J, Steinkemper H, Hermle M. Molybdenum and tungsten oxide: High work function wide band gap contact materials for hole selective contacts of silicon solar cells. Sol. Energy Mater. Sol. Cells, 2015; 142, 34-41.

[5] Yang X, Bi Q, Ali H, Davis K, Schoenfeld WV, Weber K. High-performance TiO_2-based electron selective contacts for crystalline silicon solar cells. Adv. Mater. 2016; 28; 5891-5897.

[6] Avasthi S, McClain WE, Man G, Kahn A, Schwartz J, Sturm JC. Hole-blocking titanium-oxide/silicon heterojunction and its application to photovoltaics. Appl. Phys. Lett. 2013; 102; 203901-1-203901-4.

[7] Nagamatsu KA, Avasthi S, Sahasrabudhe G, Man G, Jhaveri J, Berg AH, Schwartz J, Kahn A, Wagner S, Sturm JC. Titanium dioxide/silicon hole-blocking selective contact to enable doubleheterojunction crystalline silicon-based solar cell. Appl. Phys. Lett. 2015; 106; 123906-1-123906-5.

[8] Liao B, Hoex B, Aberle AG, Chi D, Bhatia CS. Excellent c-Si surface passivation by low-temperature atomic layer deposited titanium oxide. Appl. Phys. Lett. 2014; 104; 253903-1-253903-4.

[9] Cui J, Allen T, Wan Y, Mckeon J, Samundsett C, Yana D, Zhang X, Cui Y, Chen Y, Verlinden P, Cuevas A. Titanium oxide: A re-emerging optical and passivating material for silicon solar cells. Sol. Energy Mater. Sol. Cells; 2016; 158; 115-121.

[10] Sinton RA, Cuevas A. Appl. Phys. Lett. 1996; 69; 2510-2512.

[11] Sinton RA, Cuevas A. A quasi-steady-state open-circuit voltage method for solar cell characterization. Proceedings of the 16th European Photovoltaic Solar Energy Conference, 2000. p. 1152-1155.

[12] Heilig K. Determination of surface properties by means of large signal photovoltage pulses and the influence of trapping. Surf. Sci. 1974; 44; 421-437.

[13] Leenderts C, Mingirulli N, Schulze TF, Kleider JP, Rech B, Korte L. Discerning passivation mechanisms at a-Si:H/c-Si interfaces by means of photoconductance measurements. Appl. Phys. Lett.; 2011; 98; 202108-1-202108-3.

[14] Bivour M, Reusch M, Schroer S, Feldmann F, Temmler J, Steinkemper H, Hermle M. Doped layer optimization for silicon heterojunctions by injection-level-dependent open-circuit voltage measurements. IEEE J. Photovoltaics; 2014; 4; 566-574.

[15] Glunz SW, Nekarda J, Mäckel H, Cuevas A. Analyzing back contacts of silicon solar cells by suns-V_{oc} measurements at high illumination densities. Proceedings of the 22nd European Photovoltaic Solar Energy Conference; 2007. p.849-853.

[16] CRC Handbook of Chemistry and Physics (92nd ed.); 12–124.

[17] Klein A, Körber C, Wachau A, Säuberlich F, Gassenbauer Y, Schafranek R, Harvey SP, Mason TO. Surface potentials of magnetron sputtered transparent conducting oxides. Thin Solid Films; 2009; 518; 1197-1203.

[18] Allen TG, Zheng P, Vaughan B, Barr M, Wan Y, Samundsett C, Bullock J, Cuevas A. Low resistance TiO_2-passivated calcium contacts to for crystalline silicon solar cells. Proceedings of the 43rd IEEE Photovoltaic Specialists Conference; 2016. p. 230-233.